

## THERMAL BEHAVIOUR OF EDGE-LOADED DISKS MADE FROM POLYSTYRENE/ NATURAL RUBBER

## TERMIČKO PONAŠANJE IVIČNO OPTEREĆENIH DISKOVA OD POLISTIRENA/ PRIRODNE GUME

Originalni naučni rad / Original scientific paper  
Rad primljen / Paper received: 15.10.2024  
<https://doi.org/10.69644/ivk-2026-01-0065>

Adresa autora / Author's address:  
Department of Mathematics, ICFAI University Himachal Pradesh,  
India P. Thakur <https://orcid.org/0000-0001-8119-2697>,  
\*email: [pankaj\\_thakur15@yahoo.co.in](mailto:pankaj_thakur15@yahoo.co.in)

### Keywords

- load
- disk
- yielding
- polystyrene
- rubber

### Abstract

*This study examines the thermal behaviour of edge-loaded disks composed of polystyrene and natural rubber under varying temperatures ( $T = 0$  and  $T = 0.5$ ). The relationship between angular speed and radius ratio is analysed, revealing that natural rubber disks require higher angular speeds for initial yielding and plastic deformation compared to polystyrene. As the radius ratio increases, angular speed decreases, especially in fully plastic conditions. Elevated temperatures enhance angular speeds for both materials, indicating improved performance. These findings highlight the critical impact of material composition and thermal conditions on the mechanical response of rotating disks, offering valuable insights for engineering applications involving composites.*

### INTRODUCTION

Thermal behaviour of materials plays a critical role in their structural performance, especially when subjected to mechanical loads and temperature variations. This research focuses on the thermal behaviour of edge-loaded disks made from polystyrene and natural rubber, two distinct materials with contrasting thermal and mechanical properties. Polystyrene, a widely used thermoplastic, is known for its rigidity, low thermal expansion, and high thermal conductivity, making it suitable for applications requiring dimensional stability. In contrast, natural rubber, with its elasticity, flexibility, and high thermal expansion, is commonly used in applications where deformation and resilience are critical. When these two materials are combined in a composite disk and subjected to edge loading, their interaction under thermal stress presents a unique case for analysis. The study of thermal stresses in such disks is essential for applications where materials undergo significant temperature changes, such as in automotive components, aerospace parts, and industrial machinery. Understanding the stress distribution and deformation patterns can help improve material selection, design, and performance in environments where both rigidity and flexibility are required. This research aims to provide insights into the behaviour of polystyrene-natural rubber composites under thermal and mechanical loads,

### Ključne reči

- opterećenje
- disk
- tečenje
- polistiren
- guma

### Izvod

*U ovom radu proučavamo termičko ponašanje ivično opterećenih diskova sačinjenih od polistirena i prirodne gume u uslovima promenljive temperature ( $T = 0$  i  $T = 0.5$ ). Analizira se veza između ugaone brzine i odnosa poluprečnika, gde diskovi od prirodne gume zahtevaju veće ugaone brzine za nastupanje tečenja i plastične deformacije u odnosu na polistiren. Sa porastom odnosa poluprečnika, ugaona brzina opada, posebno u uslovima potpune plastičnosti. Povišena temperatura povećava ugaonu brzinu kod obe vrste materijala, ukazujući na poboljšanje performansi. Ova otkrića naglašavaju kritične uticaje vrste materijala i termičkih uslova na mehaničko ponašanje rotirajućih diskova, čime se stiču bitna saznanja u inženjerstvu i primeni kompozitnih materijala.*

contributing to the development of more efficient and durable composite materials for various engineering applications. The study of thin rotating disks made from isotropic materials has been thoroughly examined by Sokolnikoff /1/ and Timoshenko and Goodier /2/ in the context of elastic behaviour, while Chakrabarty /3/ and Heyman /4/ addressed the plastic range. Their approach to the fully plastic state does not rely on the plane stress condition; thus, it is possible to determine the required stresses and angular velocity for the disk to reach full plasticity without assuming plane stress (i.e.,  $T_{zz} = 0$ ). In contrast, Gupta and Shukla /5/ provided an alternative solution for the fully plastic state utilising Seth's transition theory alongside the plane stress condition.

### OBJECTIVE OF THE STUDY

The objective of this study is to investigate the thermal behaviour of edge-loaded disks made from polystyrene and natural rubber. By analysing the interaction between these two materials under thermal and mechanical loading conditions, the research aims to understand stress distribution, deformation patterns, and overall performance. The study seeks to explore how the unique properties of polystyrene and natural rubber affect thermal stress behaviour, particularly in applications where temperature fluctuations are prevalent. Ultimately, the findings aim to provide valuable insights

for optimising the design and material selection of composite disks in various engineering applications, ensuring enhanced durability and efficiency.

### GOVERNING EQUATIONS

A thin annular disk made of polystyrene and natural rubber, characterised by a constant density and defined by a central bore radius  $r_i$  and an outer radius  $r_0$ , is examined (Fig. 1). This disk, composed of uniform material, is subjected to edge loading while rotating at an angular speed about an axis perpendicular to its plane. With a constant and sufficiently small thickness, the disk operates under a state of plane stress, implying that the axial stress  $T_{zz}$  is negligible. The temperature at the central bore of the disk is denoted by  $T_0$ .

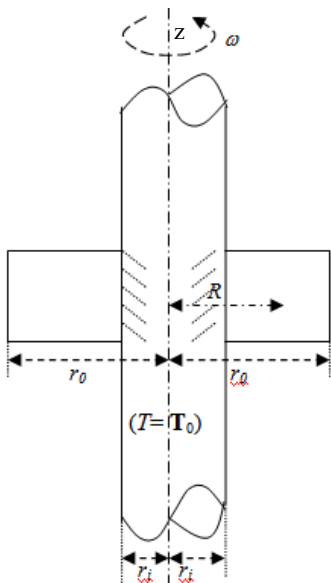


Figure 1. Geometry of the disk.

The equation of stress is given by Thakur, /8/:

$$\begin{aligned} T_{rr} &= \frac{2\mu}{n} \left[ 3-2c-\beta^n \left\{ 1-c+(2-c)(P+1)^n + \frac{nc\xi T}{2\mu\beta^n} \right\} \right], \\ T_{\theta\theta} &= \frac{2\mu}{n} \left[ 3-2c-\beta^n \left\{ 2-c+(1-c)(P+1)^n + \frac{nc\xi T}{2\mu\beta^n} \right\} \right], \\ T_{r\theta} &= T_{\theta z} = T_{zr} = T_{zz} = 0, \end{aligned} \quad (1)$$

where:  $c = 2\mu/\lambda + 2\mu$ . All equilibrium equations are fulfilled, with the exception of:

$$\frac{d}{dr}(rT_{rr}) - T_{\theta\theta} + \rho\omega^2 r^2 = 0. \quad (2)$$

The boundary conditions are as follows:

$$\begin{aligned} T_{rr} &= 0, T = T_0 \text{ at } r = r_i; \quad T_{rr} = L_0, \Theta = 0 \text{ at } r = r_0 \\ \text{and} \quad T &= T_0 \ln(r/b)/\ln(a/b). \end{aligned} \quad (3)$$

By substituting Eqs.(1) and (3) into Eq.(2), we obtain a nonlinear differential equation expressed as:

$$\begin{aligned} (2-c)n\beta^{n+1}P(P+1)^{n-1} \frac{dP}{d\beta} &= \frac{n\rho\omega^2 r^2}{2\mu} - \frac{nc\xi \bar{T}_0}{2\mu} + \\ &+ \beta^n \left[ 1-(P+1)^n - nP\{1-c+(2-c)(P+1)^n\} \right], \end{aligned} \quad (4)$$

where:  $\bar{T}_0 = T_0/\ln(r_i/r_0)$ . According to Eq.(4), the turning points of  $\beta$  are identified as  $P = -1$  and  $\pm\infty$ .

### SOLUTION

It has been demonstrated /5-26/ that the asymptotic solution for principal stress transitions from elastic state to the plastic state at transition point  $P \rightarrow \pm\infty$ . The transition function  $R$  is defined as follows:

$$R = \frac{n}{2\mu} [T_{\theta\theta} - c\xi T] = \left[ (3-2c) - \beta^n \{ 2-c+(1-c)(P+1)^n \} - \frac{nc\xi T}{\mu} \right]. \quad (5)$$

By performing logarithmic differentiation of Eq.(5) with respect to  $r$  and substituting the value of  $dP/d\beta$  from Eq.(4), we obtain:

$$\begin{aligned} \frac{d(\log R)}{dr} &= \frac{\beta^n \left( \frac{1-c}{2-c} \right) \times \left[ 1-(P+1)^n - n(1-c)P + \frac{n\rho\omega^2 r^2}{2\mu\beta^n} + \frac{nc\xi \bar{T}_0(3-2c)}{\mu(4-2c)\beta^n} \right] + (2-c)nP\beta^n}{r \left[ 3-2c-\beta^n \{ 2-c+(1-c)(P+1)^n \} - \frac{nc\xi T}{2\mu} \right]}. \end{aligned} \quad (6)$$

By taking the asymptotic value  $P$  from Eq.(6) and integrating, we arrive at:

$$R = Ar^{\nu-1}. \quad (7)$$

where:  $\nu = 1 - c/(2-c)$ . From Eqs.(5) and (7), we obtain:

$$T_{\theta\theta} = \left( \frac{2\mu}{n} \right) K_1 r^{\nu-1} + \frac{C\xi T_0 \ln(r/r_0)}{\log(r_i/r_0)}. \quad (8)$$

By substituting Eq.(8) into Eq.(2) and performing the integration, we obtain:

$$T_{rr} = \left( \frac{2\mu}{nv} \right) Ar^{\nu-1} + \frac{C\xi T_0 \log(r/r_0)}{\ln(r_i/r_0)} - \frac{C\xi \Theta_0}{\ln(r_i/r_0)} - \frac{\rho\omega^2 r^2}{3} + \frac{B}{r}. \quad (9)$$

By applying boundary condition Eq.(3) to Eq.(9), we obtain:

$$\begin{aligned} A &= \frac{nv}{2\mu(r_0^\nu - r_i^\nu)} \left( r_0 L_0 + \frac{\rho\omega^2}{3} [r_0^3 - r_i^3] + \frac{C\xi T_0}{\ln(r_i/r_0)} [r_i \ln(r_i/r_0) - r_i + r_0] \right), \text{ and} \\ B &= -\frac{r_i^\nu}{(r_0^\nu - r_i^\nu)} \left( r_0 L_0 + \frac{\rho\omega^2}{3} [r_0^3 - r_i^3] + \frac{C\xi T_0}{\ln(r_i/r_0)} [r_i \ln(r_i/r_0) - r_i + r_0] \right). \end{aligned}$$

By inserting the values of  $A$  and  $B$  into Eqs.(8) and (9), we arrive at:

$$\begin{aligned} T_{rr} &= \frac{r^\nu - r_i^\nu}{r(r_0^\nu - r_i^\nu)} \left( r_0 L_0 + \frac{\rho\omega^2}{3} [r_0^3 - r_i^3] + \frac{\alpha E \Theta_0}{(1-\nu)\ln(r_i/r_0)} \times \right. \\ &\times [r_i \ln(r_i/r_0) - a + b] \left. \right) + \frac{\rho\omega^2}{3r} [r_i^3 - r^3] + \frac{\alpha E T_0}{\log(r_i/r_0)(1-\nu)} \times \\ &\times \left[ \{ \ln(r/r_0) - 1 \} - \frac{r_i}{r} \{ \ln(r_i/r_0) - 1 \} \right], \end{aligned} \quad (10)$$

$$\begin{aligned} T_{\theta\theta} &= \frac{\nu r_i^{\nu-1}}{(r_0^\nu - r_i^\nu)} \left( r_0 L_0 + \frac{\rho\omega^2}{3} [r_0^3 - r_i^3] + \frac{\alpha E T_0}{\ln(r_i/r_0)(1-\nu)} \times \right. \\ &\times [r_i \ln(r_i/r_0) - r_i + r_0] \left. \right) + \frac{\alpha E (2-C) T_0 \ln(r/r_0)}{(1-\nu)\ln(r_i/r_0)}. \end{aligned} \quad (11)$$

As observed from Eq.(11),  $T_{\theta\theta}$  reaches its maximum at the internal surface; thus, yielding will occur at this surface, leading to Eq.(11) becoming:

$$|T_{\theta\theta}|_{r=a} = \frac{\nu r_i^{\nu-1}}{(r_0^\nu - r_i^\nu)} \left( r_0 L_0 + \frac{\rho \omega^2}{3} [r_0^3 - r_i^3] \right) + \frac{\alpha E T_0}{\ln(r_i/r_0)(1-\nu)} \times \\ \times [r_i \ln(r_i/r_0) - r_i + r_0] + \frac{\alpha E T_0}{(1-\nu)} \equiv Y(\text{say}),$$

and angular speed  $\omega_i$  necessary for initial yielding is given by:

$$\Omega_i^2 = \frac{\rho \omega_i^2 b^2}{Y} = \frac{3r_0^2}{(r_0^3 - r_i^3)} \left[ \frac{(r_0^\nu - r_i^\nu)}{r_i^{\nu-1} \nu} - b L_0 - \frac{\alpha E \Theta_0}{Y(1-\nu)} \right] \times \\ \times \left\{ r_i - \frac{r_i}{\ln(r_i/r_0)} + \frac{r_0}{\ln(r_i/r_0)} + \frac{(r_0^\nu - r_i^\nu)}{\nu r_i^{\nu-1}} \right\}, \quad (12)$$

where:  $L = L_0/Y$ . We introduce the following non-dimensional components as  $R = r/r_0$ ,  $R_0 = r_i/r_0$ ,  $\Omega^2 = \rho \omega^2 r_0^2/Y$ ,  $\alpha E T_0/Y = T$ ,  $\sigma_r = \tau_{rr}/Y$ ,  $\sigma_\theta = \tau_{\theta\theta}/Y$  and  $L = L_0/Y$ . Equations (10), (11), and (12) become:

$$\sigma_r = \frac{R^\nu - R_0^\nu}{R(1-R_0^\nu)} \left[ L + \frac{\Omega_i^2}{3} (1-R_0^3) + \frac{T}{\ln(R_0)(1-\nu)} \{R_0 \ln(R_0) - R_0 + 1\} \right] - \\ - \frac{\Omega_i^2}{3R} (R^3 - R_0^3) + \frac{T}{R \ln(R_0)(1-\nu)} [R(\ln R - 1) - R_0(\ln R_0 - 1)] \quad (13)$$

$$\sigma_\theta = \frac{\nu R^{\nu-1}}{(1-R_0^\nu)} \left[ L + \frac{\Omega_i^2}{3} (1-R_0^3) + \frac{T}{\ln(R_0)(1-\nu)} \{R_0 \ln(R_0) - R_0 + 1\} \right] + \\ + \frac{T \ln R}{\ln(R_0)(1-\nu)}, \quad (14)$$

$$\Omega_i^2 = \frac{3}{(1-R_0^3)} \left[ \frac{(1-R_0^\nu)}{\nu R_0^{\nu-1}} - L - \frac{T}{(1-\nu)} \right] \times \\ \times \left\{ R_0 - \frac{R_0}{\ln R_0} + \frac{1}{\ln R_0} + \frac{1-R_0^\nu}{\nu R_0^{\nu-1}} \right\}. \quad (15)$$

Equations (13), (14), and (15) provide the thermoelastic-plastic transitional stresses and angular speed for a thin rotating disk subjected to edge loading. The stresses and angular speed described by Eqs.(13) and (14) for full plasticity are given by:

$$\sigma_r = \frac{\sqrt{R} - \sqrt{R_0}}{R(1-\sqrt{R_0})} \left[ L + \frac{\Omega_f^2}{3} (1-R_0^3) + \frac{2T}{\ln(R_0)} \{R_0 \ln(R_0) - R_0 + 1\} \right] - \\ - \frac{\Omega_f^2}{3R} (R^3 - R_0^3) + \frac{2T \{ \ln(R_0) - 1 \}}{R \ln(R_0)} [R - R_0], \quad (16)$$

$$\sigma_\theta = \frac{1}{2\sqrt{R}(1-\sqrt{R_0})} \left[ L + \frac{\Omega_f^2}{3} (1-R_0^3) + \frac{2T}{\ln(R_0)} \times \right. \\ \left. \times \{R_0 \ln(R_0) - R_0 + 1\} \right] + \frac{2T \ln R}{\ln(R_0)}. \quad (17)$$

From Eq.(11) the angular speed  $\omega_f > \omega_i$  for which the disk becomes fully plastic  $\nu = 0.5$  at  $r = b$  is given by:

$$\Omega_f^2 = \frac{\rho \omega_f^2 b^2}{Y} = \frac{3}{1-R_0^3} \left[ 2(1-\sqrt{R_0}) - \sigma_0 - \frac{2T_1}{\ln R_0} (R_0 \ln R_0 - R_0 + 1) \right] \quad (18)$$

where:  $\omega_f = \frac{1}{r_0} \Omega_f (Y/\rho)^{1/2}$ .

## Validation of results

The presented results in Eqs.(13)-(18) are the same by neglecting load and thermal conditions from the results given by Thakur, /8/.

## RESULTS AND DISCUSSION

To compute the stresses and angular speed from the analysis, the following values are used: Poisson's ratio is set at  $\nu = 0.33$  for polystyrene (PS),  $\nu = 0.5$  for natural rubber (NR),  $L = 0, 0.1$ , and  $T = 0$  and  $0.5$ , respectively. The parameters chosen include an inner radius  $r_i = 1$  mm, an outer radius  $r_0 = 2$  mm, and a reference radius  $R_0 = 0.5$ . The graphs in Fig. 2 illustrate the relationship between angular speed and the radius ratio at two different temperature conditions,  $T = 0$  and  $T = 0.5$ . In summary, the analysis of angular speed versus radius ratio at different thermal conditions reveals significant insights into the behaviour of edge-loaded disks made from polystyrene and natural rubber. At  $T = 0$ , the results indicate that natural rubber disks require higher angular speeds for initial yielding and fully plastic deformation compared to polystyrene, reflecting the distinct mechanical properties of these materials. As the radius ratio increases, the angular speed decreases, particularly under fully plastic conditions. When the temperature is elevated to  $T = 0.5$ , a similar trend is observed, but the overall angular speed values

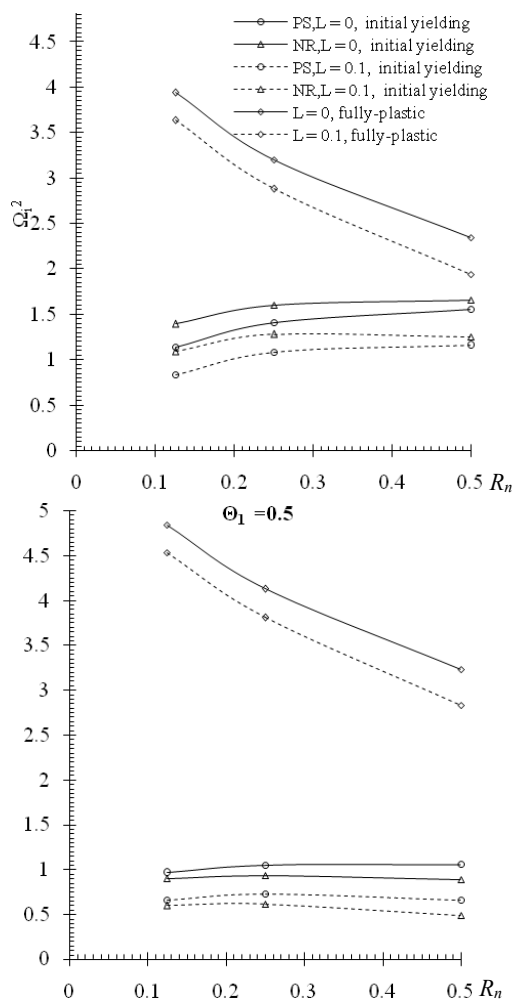


Figure 2. Angular speed vs. radii ratio at  $T = 0$  and  $T = 0.5$ .

are higher, suggesting that increased thermal conditions enhance the performance of both materials. These findings underscore the crucial influence of material composition and thermal effects on the mechanical response of thin rotating disks, providing valuable guidance for engineering applications involving composite materials. The graph in Fig. 3 illustrates the relationship between angular speed ( $\Omega_i^2$ ) and variable  $L$  for both polystyrene (PS) and natural rubber (NR) disks under varying thermal conditions. The results indicate that: at  $T = 0$  both materials exhibit higher angular speeds during initial yielding compared to their performance at  $T = 0.5$ . As  $L$  increases, there is a noticeable decrease in angular speed for both materials, particularly in the fully plastic condition. The trends reveal that natural rubber disks require lower angular speeds for initial yielding than polystyrene when subjected to higher thermal conditions. This behaviour underscores the significant influence of both material composition and temperature on the mechanical performance of edge-loaded disks, providing critical insights for their application in engineering contexts. Overall, the data emphasise the distinct performance characteristics of polystyrene and natural rubber in terms of angular speed under varying conditions.

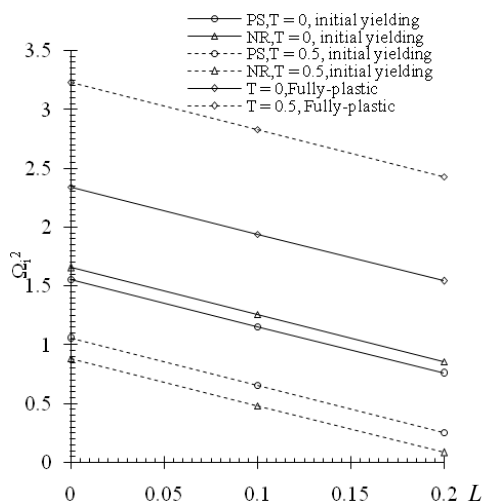


Figure 3. Angular speed vs.  $L$ .

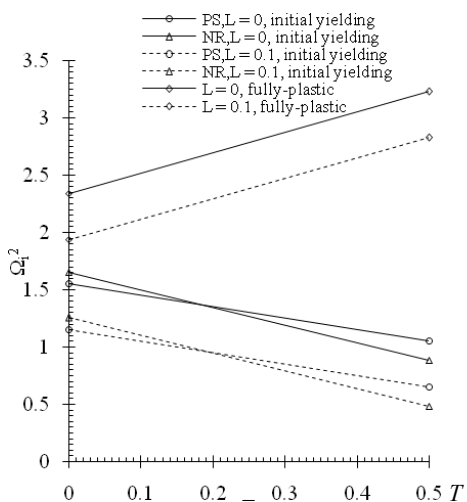


Figure 4. Angular speed vs.  $T$ .

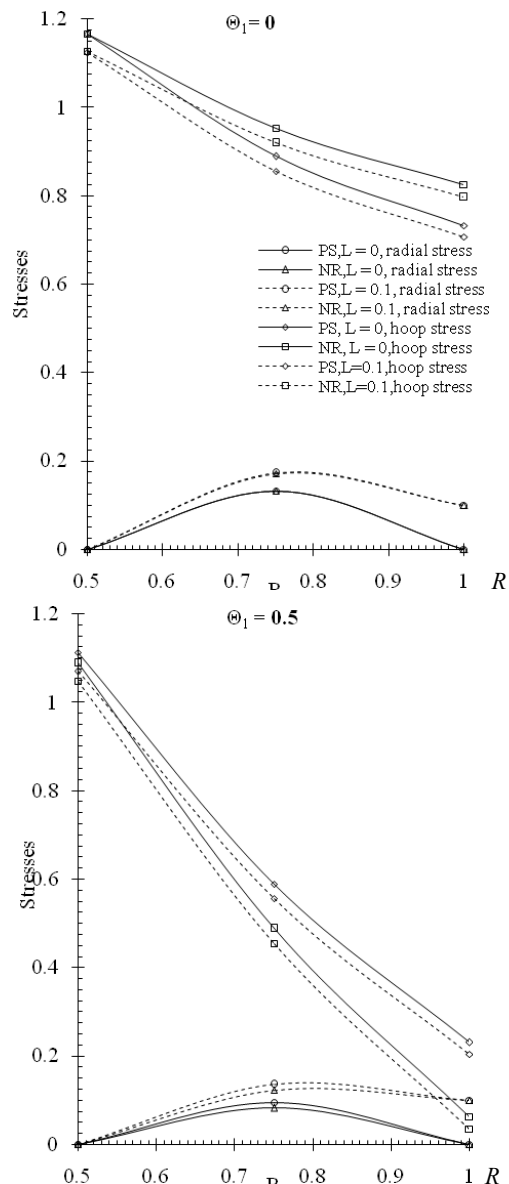


Figure 5. Stress distribution vs. radius  $R$ .

The graph in Fig. 4 illustrates the relationship between angular speed squared ( $\Omega_i^2$ ) and parameter  $T$  for different material conditions and loading scenarios. The graph includes several curves representing different configurations: PS (perfectly solid) and NR (non-rigid), with  $L = 0$  or  $L = 0.1$ , under initial yielding and fully plastic conditions. It shows that as  $T$  increases, the angular speed-squared changes depending on the material properties and loading conditions. The curves for  $L = 0$  exhibit different slopes compared to those for  $L = 0.1$ , indicating the influence of this parameter on mechanical behaviour. The fully plastic conditions typically result in lower angular speeds compared to the initial yielding cases, suggesting that material deformation significantly affects the system's rotational dynamics. Figure 5 presents a comprehensive view of stress distribution versus radial position ( $R$ ) for various material conditions and parameters, comparing two scenarios:  $T = 0$  and  $T = 0.5$ . The graphs illustrate radial and hoop stresses for both perfectly solid (PS) and non-rigid (NR) materials, with load parameters

$L = 0$  and  $L = 0.1$ . In the upper Fig. 5, when  $T = 0$ , radial stress decreases with increasing radius, with PS materials exhibiting higher stress values than NR materials. Hoop stress, in contrast, initially increases and then decreases across the radial distance. In the lower Fig. 5, when  $T = 0.5$ , a similar trend is observed, but with generally higher stress values across both material types. The influence of the load parameter  $L$  is notable in both upper and lower Fig. 5, particularly with  $L = 0.1$ , which results in distinct stress behaviours compared to  $L = 0$ .

## CONCLUSIONS

The main findings are:

- the edge-loaded disks made from polystyrene and natural rubber exhibit distinct behaviours under different thermal conditions;
- natural rubber disks require higher angular speeds for initial yielding and fully plastic deformation compared to polystyrene;
- fully plastic conditions generally result in lower angular speeds than initial yielding conditions, highlighting the significant effect of material deformation on rotational dynamics;
- radial stress decreases with increasing radius; PS materials have higher stress values than NR materials;
- hoop stress initially increases and then decreases across the radial distance.

## ACKNOWLEDGEMENTS

This research article is especially dedicated to Prof. Dr. Aleksandar Sedmak (Editor-in-chief Emeritus), Prof. Zoran Radaković (editor-in-chief) of *Structural Integrity and Life* journal and the Society for Structural Integrity and Life 'Prof. Dr. Stojan Sedmak'/IMS Institute, Serbia.

## REFERENCES

1. Sokolnikoff, I.S., *Mathematical Theory of Elasticity*, 2<sup>nd</sup> Ed., McGraw Hill Book Co., New York, 1956.
2. Timoshenko, S.P., Goodier, J.N., *Theory of Elasticity*, 3<sup>rd</sup> Ed., McGraw-Hill Book Co., New York, USA, 1970.
3. Chakrabarty, J., *Theory of Plasticity*, McGraw-Hill, New York, 1987.
4. Heyman J., (1958), *Plastic design of rotating discs*, Proc. Inst. Mech. Eng. 172(1): 531-547. doi: 10.1243/PIME\_PROC\_1958\_172\_045
5. Gupta, S.K., Shukla, R.K. (1994), *Elastic-plastic transition in a thin rotating disc*, Ganita, 45(2): 78-85.
6. Seth, B.R. (1962), *Transition theory of elastic-plastic deformation, creep and relaxation*, Nature, 195: 896-897. doi: 10.1038/195896a0
7. Seth, B.R. (1966), *Measure concept in mechanics*, Int. J Non-Linear Mech. 1(1): 35-40. doi: 10.1016/0020-7462(66)90016-3
8. Thakur, P., *Some problems in elastic-plastic and creep transition*, Ph.D. Thesis, Dept. of Mathematics and Statistics, Himachal Pradesh University, Shimla, India, 2006  
<https://shodhganga.inflibnet.ac.in/handle/10603/121294>
9. Thakur, P. (2013), *Creep transition stresses of orthotropic thick-walled cylinder under combined axial load under internal pressure*, Facta Universities Ser.: Mech. Eng. 11(1): 13-18.
10. Sethi, M., Thakur, P., Singh, H.P. (2019), *Characterization of material in a rotating disc subjected to thermal gradient by using Seth transition theory*, Struct. Integr. Life, 19(3): 151-156.

11. Thakur, P., Shahi, S., Singh, S.B., Sethi, M. (2019), *Elastic-plastic stress concentrations in orthotropic composite spherical shells subjected to internal pressure*, Struct. Integr. Life, 19(2): 73-77.
12. Thakur, P., Sethi, M. (2019), *Lebesgue measure in an elasto-plastic shell*, Struct. Integr. Life, 19(2): 115-120.
13. Temesgen, A.G., Singh, S.B., Thakur, P. (2020), *Modelling of elastoplastic deformation of transversely isotropic rotating disc of variable density with shaft under a radial temperature gradient*, Struct. Integr. Life, 20(2): 113-121.
14. Thakur, P., Kumar, N., Sukhvinder (2020), *Elasto-plastic density variation in a deformable disk*, Struct. Integr. Life, 20 (1): 27-32.
15. Thakur, P., Gupta N., Gupta K., Sethi, M. (2020), *Elastic-plastic transition in an orthotropic material disk*, Struct. Integr. Life, 20(2): 169-172.
16. Thakur, P., Chand, S., Sukhvinder, et al. (2020), *Density parameter in a transversely and isotropic disc material with rigid inclusion*, Struct. Integr. Life, 20(2): 159-164.
17. Thakur P., Sethi, M., Gupta, K., Bhardwaj R.K. (2021), *Thermal stress analysis in a hemispherical shell made of transversely isotropic materials under pressure and thermo-mechanical loads*, Zeitschrift für angewandte Mathematik und Mechanik, 101(12): e202100208. doi: 10.1002/zamm.202100208
18. Thakur, P., Sethi, M., Kumar, N., et al. (2021), *Analytical solution of hyperbolic deformable disk having variable density*, Mech. Solids, 56(6): 1039-1046. doi: 10.3103/S0025654421060194
19. Kumar, N., Thakur, P. (2021), *Thermal behaviour in a rotating disc made of transversely isotropic material with rigid shaft*, Struct. Integr. Life, 21(3): 217-223.
20. Thakur, P., Kumar, N., Gupta, K. (2022), *Thermal stress distribution in a hyperbolic disk made of rubber/brass material*, J Rubber Res. 25(1): 27-37. doi: 10.1007/s42464-022-00147-6
21. Chand, S., Sood, S, Thakur, P., Gupta, K. (2023), *Elasto-plastic stress deformation in an annular disk made of isotropic material and subjected to uniform pressure*, Struct. Integr. Life, 23 (1): 61-64.
22. Singh, N., Kaur, J., Thakur, P., Murali, G. (2023), *Structural behaviour of annular isotropic disk made of steel/copper material with gradually varying thickness subjected to internal pressure*, Struct. Integr. Life, 23(3): 293-297.
23. Sukhvinder, Gulial, P., Pathania, D.S., et al. (2024), *Comparative study of creep in a disk made of rubber/copper material and fitted with rigid shaft*, Struct. Integr. Life, 24(2): 159-166. doi: 10.69644/ivk-2024-02-0159
24. Kumar, S., Thakur, P., Sood, S., et al. (2024), *Transversely isotropic elastoplastic behaviour in a mechanically loaded rotating disk*, Struct. Integr. Life, 24(2): 167-171. doi: 10.69644/ivk-2024-02-0167
25. Sukhvinder, Gulial, P., Pathania, D.S., et al. (2024), *Thermal stress distribution in a tube of natural rubber/polyurethane material and subjected to internal pressure and mechanical load*, Struct. Integr. Life, 24(2): 151-158. doi: 10.69644/ivk-2024-02-0151
26. Singh, A., Gulial, P., Thakur, P. (2024), *Exploring the effective stress behavior of internally pressurized cylinders with varying density*, ZAMM - J Appl. Math. Mech. 104(8): e202400254. doi: 10.1002/zamm.202400254

© 2026 The Author. Structural Integrity and Life, Published by DIVK (The Society for Structural Integrity and Life 'Prof. Dr Stojan Sedmak') (<http://divk.inovacionicentar.rs/ivk/home.html>). This is an open access article distributed under the terms and conditions of the [Creative Commons Attribution-NonCommercial-NoDerivatives 4.0 International License](https://creativecommons.org/licenses/by-nc-nd/4.0/)